Scientific Data

https://doi.org/10.1038/s41597-026-06862-8

Article in Press

An integrated database of combustion properties of metallic materials

Received: 10 September 2025

Accepted: 6 February 2026

Cite this article as: Wang, P., Ke, H., Xue, Y. An integrated database of combustion properties of metallic materials. *Sci Data* (2026). https://doi.org/10.1038/s41597-026-06862-8

Penglin Wang, Huibin Ke & Yunfei Xue

An integrated database of combustion properties of metallic materials

Penglin Wang[1], Huibin Ke[1,2,3*], Yunfei Xue[1,2,3]

[1] School of Materials Science and Engineering, Beijing Institute of Technology, Beijing, China.

[2] Yangtze Delta Region Academy of Beijing Institute of Technology, Jiaxing, Zhejiang, China.

[3] National Key Laboratory of Science and Technology on Materials Under Shock and Impact, Beijing, China

*Correspondence: kehuibin@bit.edu.cn

Abstract: Metal combustion, which is fundamentally a rapid exothermic redox reaction with oxygen, governs critical applications from aerospace propulsion to structural fire safety. Understanding key combustion metrics including combustion enthalpy, ignition temperature, ignition delay time, combustion rate, and threshold pressure is essential for designing fire-resistant alloys or high-energy propellants. This work establishes a comprehensive database of 725 curated data points extracted from 45 publications, mainly encompassing pure metals, Al-based, Ti-based, Mg-based, Fe-based alloys and multi-component alloys. Each data entry integrates combustion metrics with alloy composition and critical experimental metadata, such as sample geometry, oxygen partial pressure and test method. By integrating scattered literature data into a unified framework with standardized parameters, this work provides a foundation for data-driven discovery of next-generation materials with tailored combustion performance.

Keywords: Metal combustion; ignition; flammability; materials informatics

Background & Summary

Combustion performance is a fundamental property of metallic materials, influencing both their practical applications and safety considerations. Aluminum alloys, for instance, are widely employed as additives in propellants due to their high energy density [1,2], where rapid, controlled combustion is desirable. To maximize their energy release, researchers have explored strategies such as particle size optimization and alloying element modification to improve the ignition and combustion performance of Al-based additives [3,4]. Conversely, the propensity of metallic materials to ignite under certain conditions can lead to catastrophic mechanical failures. Titanium and magnesium alloys, for example, known for their high specific strength, low density and corrosion resistance, are extensively utilized in automotive and aerospace industries [5-11]. However, their susceptibility to combustion at elevated temperatures, leading to fire accidents, poses severe safety risks, limiting their applications [10,12]. Consequently, extensive research has been conducted to understand the ignition and combustion behaviors of these alloys for both performance enhancement and hazard mitigation [7,10-15]. Despite these divergent objectives, both scenarios necessitate a fundamental understanding of metal ignition and combustion mechanisms.

Fundamentally, metal combustion is a rapid exothermic redox reaction, typically with oxygen in the surrounding environment. The process begins when a metal surface is exposed to an oxidizing atmosphere, forming a thin oxide layer through the reaction $M + \frac{x}{2}O_2 \rightarrow MO_x$ (ΔH_c<0). This initial oxidation serves a dual purpose: it releases thermal energy while simultaneously creating a diffusion barrier that temporarily inhibits further reaction, which causes ignition delay. However, as oxidation progresses, localized hotspots emerge due to defects caused by thermal stresses between metal and its oxide, and the heat release rate increases, which will further destabilize the oxide layer. As the rate of heat accumulation surpasses the rate of heat dissipation, the material can rapidly reach its ignition temperature, leading to combustion [10,11,15,16]. Once ignited, the combustion may proceed through condensed, molten or gas phase reactions. The combustion front propagates as a wave, with continuous oxide formation and breakdown sustaining the reaction until either the metal is fully consumed or the heat flux drops below the threshold for self-sustained burning.

Combustion properties are characterized by both thermodynamic and kinetic metrics. Thermodynamically, combustion enthalpy (ΔH_c) defines the theoretical highest energy release, while kinetic properties include ignition and flammability parameters. Key kinetic evaluation metrics include:

- Ignition temperature: Lowest temperature measured experimentally at which there occurs the most rapid rate of change with time of both light intensity and sample temperature [17-20].
- Ignition delay time: Time duration between exposure to heat source and ignition [1,21].
- Combustion/regression rate: Speed of flame propagation or material consumption, which can be evaluated with either length/volume rate or mass rate [22,23].
- Threshold pressure: The minimum pressure at a specified oxygen concentration and ambient temperature that supports self-sustained combustion of the entire standard sample, which is a cylindrical rod with 3.2 mm diameter and 150 mm length according the ASTM G-124 standard [24].

The combustion behaviors of metallic materials are not only sensitive to alloy composition and oxide characteristics, such as Pilling-Bedworth ratio [25] but also sensitive to external experimental parameters including testing methods, environmental conditions and specimen geometries. For example, ignition test results demonstrate that increasing the heating rate significantly raises the measured ignition temperature of magnesium alloys [10,11,15]. Similarly, Lee *et al*. [26] used different test methods to study the ignition temperature of AM60/AZ91+*x*CaO alloys and found that values obtained by chip ignition test were significantly lower than those measured by differential thermal analysis (DTA). Besides testing methods, specimen geometry is also a critical factor influencing the results. Feng[3] investigated the ignition delay time of aluminum powders with varying particle sizes under different environmental oxygen concentrations. The results indicate that as particle size increases, the ignition delay time increases. For bulk samples, sample geometry also plays an important role in the experimental results measured. However, various specimen geometry including bar, block, and chip were used in previous works, as illustrated in Fig. 1. All of these variations make the direct comparative studies across different alloys challenging.

Fig. 1 Distribution of size and geometry of measured bulk samples for combustion metrics [18,27-45]

In this study, we created a comprehensive database with combustion metrics that could be fed into machine learning (ML) based models to allow for exploration of the compositional space beyond what was used to create the current database. To our knowledge, this is the first published database of this type. A high level of overview of the dataset is shown in Fig. 2. The data were collected from 45 publications comprising 725 data points, with materials falling into 13 material classes. There are 6 datasets reporting a total of 5 different combustion metrics, e.g. combustion enthalpy, ignition temperature, ignition delay time, combustion rate, combustion temperature and threshold pressure. The combustion performance database was designed to support ML-based models, enabling the exploration of material composition spaces and the development of empirical models. The database comprises a wide range of experimental conditions, such as sample sizes, oxygen pressures, and testing methodologies, which previously varied significantly across studies. This standardized presentation of experimental conditions and results facilitates pattern recognition and predictive modeling, which not only facilitates the development of calculable matrices that could shed light on the fundamental physical processes that govern combustion performance but also supports the development of predictive ML models for alloy design.

Fig. 2 A schematic overview of the dataset.

Methods

Among the over 160 literature sources reviewed, many did not provide the necessary combustion properties or loading path information. Such data points were not included in our dataset. Ultimately, we retained data from 45 paper [3,4,12,18,21-23,27-64], spanning research from 1950 to 2024, with approximately 70% being published after 2010. Relevant combustion properties data were extracted through multiple approaches: (1) Direct collection from reported values in tables and text; (2) digitization of graphical data using WebPlotDigitizer software(https://automeris.io/)[65] ; (3) calculation of derived parameters when sufficient experimental details were provided. The final curated dataset encompasses 725 individual records across 13 material classes, capturing 5 key combustion metrics, e.g. combustion enthalpy, ignition temperature, ignition delay time, combustion rate and threshold pressure. Each data point includes both the measured combustion properties and associated experimental metadata to ensure proper contextual interpretation.

For combustion rate data, we implemented a standardized processing approach to account for variations in sample sizes across different studies. The volumetric combustion rate (V), when not directly reported, was calculated from reported linear rates (v) using the following formula:

$$V = v\,\pi(\frac{d}{2})^2 \quad (1)$$

where d is the diameter of bar sample specified in the original literature. Please note the radius were calculated from the nominal diameter reported in the literature, which may introduce errors to the calculated volumetric combustion rate. This normalization enables meaningful comparison of combustion rates across different experimental configurations.

Data Record

The dataset is provided as an Excel spreadsheet hosted on Figshare[66] and on github[67]. It contains six individual worksheets, each corresponding to a specific combustion metric: combustion enthalpy, ignition temperature, ignition delay time, combustion rate (volumetric), combustion rate (mass), and threshold pressure.

Data entries include string and numeric data types. Text data such as test method and promoter in PIC test are stored as strings. The element compositions and combustion metrics are defined as numbers, and other numeric data such as sample parameters, oxygen pressure, and experimental temperature are stored in the form of a numeric array. An individual record is defined as having a unique composition, property, experimental condition and reference combination. This architecture enables both discrete analysis of individual measurements and systematic evaluation of parameter dependencies.

Each worksheet contains rows representing individual experimental measurements and columns describing alloy composition, combustion properties, and experimental conditions. Missing values are indicated as blank cells. Units are provided in the column headers.

The column headings include:

- Alloy name (string)

– Elemental composition (wt.%, numeric)

– Oxygen pressure (MPa, numeric): The gas environment is a critical factor in controlling the ignition and combustion characteristics of alloy samples. For the reaction of alloys with oxygen, oxygen concentration or partial pressure also controls the reaction process.

– X_{eff}: X_{eff} is the effective molar fraction of the oxidant in the post-combustion gas changed by varying air and oxygen flow rates. Data of X_{eff} are related to ignition delay time data in this database. The effective oxidizer mole fraction is defined by:

$$X_{eff} = X_{O_2} + 0.6H_2O + 0.22X_{CO_2} \quad (2)$$

– H_2O pressure, N_2 pressure, Ar pressure (MPa, numeric): These columns describe the gas content of reaction atmosphere when testing ignition delay time.

– Test method: Basically, test methods compile promoted ignition-combustion test (PIC), furnace-heating test, premixed flame test and the minority of laser-ignition test. Combustion metrics, especially ignition delay time and ignition temperature, can be affected by test method, which should be considered if these inputs are combined.

An example section of the dataset of volumetric combustion rate is shown in Table 1, and the other datasets follow the same or a very similar format. The reference number corresponds to the references in the final tab of the dataset.

Table 1 A section of combustion rate dataset. The full elemental composition includes the following elements: Ti, Al, Cu, Si, V, Cr, Zr, Mg, Ni, Fe.

Alloy Name	Composition (wt.%)				Oxygen pressure (MPa)	Combustion Length (mm)	Combustion rate (mm/s)	Sample bar diameter (mm)	Combustion rate (mm^3/s)	Ref.
	Ti	Al	Cu	Cr						
Ti14	84.46	1.24	13.91	0	0.2	10	2.3	3.2	18.5	22
Ti14	84.46	1.24	13.91	0	0.3	20	4.4	3.2	35.2	22
Ti14	84.46	1.24	13.91	0	0.3	30	5.8	3.2	47	22
Ti14	84.46	1.24	13.91	0	0.3	40	7.2	3.2	57.5	22
Ti14	84.46	1.24	13.91	0	0.4	10	3.2	3.2	24.9	22
Ti-25V-10Cr	65	0	0	25	0.1	40	48.0	3.2	385.8	55
Ti-25V-10Cr	65	0	0	25	0.3	40	57.0	3.2	458	55
Ti-25V-15Cr	65	0	0	25	0.4	40	54.1	3.2	498.8	55

Ti-2Cu	98	0	2	0	0.1	40	6.4	1.79	51.8	[56]
Ti-2Cu	98	0	2	0	0.2	10	3.8	1.79	30.2	[56]
Ti-2Cu	98	0	2	0	0.2	20	4.8	1.79	38.5	[56]

Data overview

As illustrated in Fig. 3, the compiled dataset comprises 725 data points systematically categorized by combustion metrics. For thermodynamic property, combustion enthalpy, we include 32 data points of pure metals, and 41 data points of alloys, e.g. Al-Ni alloys and multi-component alloys. For kinetic metrics, we include a total of 652 data points of ignition delay time, ignition temperature, combustion rate and threshold pressure. Most ignition delay time data were obtained from powders, with a small portion from bulk samples; in contrast, ignition temperature data primarily derive from bulk samples, though some powder-based measurements are included. The other two kinetic metrics were measured exclusively on bulk samples. The metal categories collected for each metric are illustrated in Fig. 3.

Fig. 3 Composition of data (The number labeled is the number of data entries for each category).

Technical Validation

The data were collected when a quantification of combustion metrics was given either in number or shown in a readable figure, and enough details regarding the test method related to combustion performance were given. Furthermore, additional screening was performed by examining outliers in various statistical plots of the datasets. In Fig. 4, a comparison between the theoretical and experimental measured combustion enthalpy is presented. As can be seen from the figure, the value of theoretical combustion enthalpy is systematically lower than experimental combustion heat, which is expected due to factors rooted in the differences between idealized models and real combustion environments.

Fig. 4 Theoretical and experimental combustion enthalpy [50].

Fig. 5 presents the screening of data regarding ignition metrics, including ignition temperature and ignition delay time. As illustrated in Fig. 5 (a), there is a positive relation between ignition temperature and ionization energy for pure metals[46,68]. In Fig. 5 (b), a relation was found between the solute oxide melting temperature[69] and ignition temperature in Mg alloys[27-29]. All the samples are cut into bulks, where heat source centered. When adding solutes with low oxide melting temperature, the ignition temperature of Mg alloys is lower than pure Mg. Conversely, when the melting point of the solute oxide exceeds a certain threshold, the corresponding ignition point is higher than that of pure Mg. Fig. 5(c) shows the ignition delay time of Al and Al-Mg particles affected by particle size and effective molar oxidant fraction (X_{eff}), and clear trends could be observed for both particle size and X_{eff} on the ignition delay time[3,53].

Fig. 5 Ignition metrics data validation by screening data with various internal and external factors. (a) Ignition temperature of pure metals as a function of ionization energy [46,68]; (b) Ignition temperature of lumped Mg alloys [27-29] as a function of oxide melting temperature of the solute metal in Mg alloys[69] (Horizontal axis representing the melting point of the oxide corresponding to the solute, and the dashed line indicating the ignition temperature of pure Mg); (c) Ignition delay time of particles by screening effect of particle size and effective molar oxidant fraction (X_{eff}) [3,53]; (d) Ignition delay time of Cu with different ignition promoters [21,54].

Fig. 6 presents the screening analysis of flammability datasets, focusing on combustion rates and threshold pressure measurements. As can be seen from the figures, the data demonstrate expected variations correlated with alloy composition, sample dimensions and oxygen pressure. When the experimental conditions are the same, results for alloys within the same material category consistently cluster within narrow ranges, confirming the internal consistency of the compiled data. This systematic behavior validates the database's reliability for comparative analysis across material systems.

Fig. 6 Screening of flammability datasets. (a) Combustion rate of Ti alloys [22,55,56], Cu-Zr alloys [57] and Al-Ni [48]; (b)Zoom-in of part of the collected data in (a); (c) Comparison of combustion rates across various alloy category; (d) Mass combustion rate of Ti-*x*Cu alloys with variations of Cu composition and O_2 proportion [23,59]; (e)Threshold pressure data of various alloys measured based on ASTM G-124 [49,70].

Data Availability

The dataset supporting this study is publicly available on Figshare at DOI: 10.6084/m9.figshare.29966602 and on github (https://github.com/wpl2000/CombustionData)

Code availability

No custom code was developed for the generation or processing of this dataset.

Acknowledgments

This work was financially supported by the YEQISUN Joint Funds of the National Natural Science Foundation of China (Grant No. U2241234).

Author Contributions

Penglin Wang: data curation, technical validation, visualization, writing – original draft preparation, writing – review and editing. Huibin Ke: concept, technical validation, writing – original draft preparation, writing – review and editing, supervision, funding acquisition. Yunfei Xue: supervision, writing – review and editing, funding acquisition.

Competing Interests

The authors declare no competing interests.

References

1. Feng, Y., Xia, Z., Huang, L. & Ma, L. Ignition and combustion of a single aluminum particle in hot gas flow. *Combustion and Flame* **196**, 35-44, doi:https://doi.org/10.1016/j.combustflame.2018.05.010 (2018).

2. Feng, Y., Xia, Z., Huang, L. & Ma, L. Effect of ambient temperature on the ignition and combustion process of single aluminium particles. *Energy* **162**, 618-629 (2018).

3. Feng, Y., Ma, L., Xia, Z., Huang, L. & Yang, D. Ignition and combustion characteristics of single gas-atomized Al–Mg alloy particles in oxidizing gas flow. *Energy* **196**, 117036 (2020).

4. Wang, W., Zou, H. & Cai, S. The Oxidation and Combustion Properties of Gas Atomized Aluminum-Boron-Europium Alloy Powders. *Propellants Explosives Pyrotechnics* **44**, 725-732, doi:10.1002/prep.201800223 (2019).

5. Busk, R. Magnesium and magnesium alloys. ASM INTERNATIONAL. (ISBN 0-87170-657-1, 1950).

6. Zhang, C. *et al.* Combustion Behavior and Microstructure of TC17 Titanium Alloy under Oxygen-Enriched Atmosphere. *Metals* **13**, 1020 (2023).

7. Boyer, R. R. An overview on the use of titanium in the aerospace industry. *Materials Science and Engineering: A* **213**, 103-114, doi:10.1016/0921-5093(96)10233-1 (1996).

8. Czerwinski, F. The oxidation behaviour of an AZ91D magnesium alloy at high temperatures. *Acta Materialia* **50**, 2639-2654, doi:10.1016/s1359-6454(02)00094-0 (2002).

9. Czerwinski, F. Oxidation Characteristics of Magnesium Alloys. *JOM* **64**, 1477-1483 (2012).

10. Czerwinski, F. Controlling the ignition and flammability of magnesium for aerospace applications. *Corrosion Science* **86**, 1-16 (2014).

11. Czerwinski, F. Overcoming barriers of magnesium ignition and flammability. *AM&P Technical Articles* **172**, 28-31 (2014).

ARTICLE IN PRESS

12. Forsyth, E. T. *et al.* Oxygen Fire Hazards in Valve-Integrated Pressure Regulators for Medical Oxygen. *J. ASTM Intl.* **6**, 285-302, doi:10.1520/JAI102296 (2009).

13. Czerwinski, F. *Magnesium alloys: corrosion and surface treatments*. (InTech, 2011).

14. Britton, L. G. *et al.* The role of ASTM E27 methods in hazard assessment part II: Flammability and ignitability. *Process Safety Progress* **24**, 12-28, doi:https://doi.org/10.1002/prs.10058 (2005).

15. Czerwinski, F. Oxidation characteristics of magnesium alloys. *JOM* **64**, 1477-1483 (2012).

16. Han, D., Zhang, J., Huang, J. F., Lian, Y. & He, G. Y. A review on ignition mechanisms and characteristics of magnesium alloys. *Journal of Magnesium and Alloys* **8**, 329-344, doi:10.1016/j.jma.2019.11.014 (2020).

17. Hou, Y., Cheng, X., Liu, S., Liu, C. & Zhang, H. Experimental study on upward flame spread of exterior wall thermal insulation materials. *Energy Procedia* **66**, 161-164 (2015).

18. Aydin, D. S., Bayindir, Z., Hoseini, M. & Pekguleryuz, M. O. The high temperature oxidation and ignition behavior of Mg–Nd alloys part I: The oxidation of dilute alloys. *Journal of Alloys and Compounds* **569**, 35-44, doi:https://doi.org/10.1016/j.jallcom.2013.03.130 (2013).

19. Farooq, M. Z., Wu, Y., Lu, L. & Zheng, M. Combustion phases of magnesium alloys based on predicted heating rate using machine learning. *Measurement* **242**, 116192, doi:https://doi.org/10.1016/j.measurement.2024.116192 (2025).

20. Laurendeau, N. & Glassman, I. Ignition temperatures of metals in oxygen atmospheres. *Combustion Science and Technology* **3**, 77-82 (1971).

21. Lynn, D., Steinberg, T., Sparks, K. & Stoltzfus, J. M. Defining the flammability of cylindrical metal rods through characterization of the thermal effects of the ignition promoter. *Journal of ASTM International* **6**, 1-12 (2009).

22. Shao, L. *et al.* Combustion Behavior and Mechanism of Ti14 Titanium Alloy. *Materials* **13**, doi:10.3390/ma13030682 (2020).

23. Chen, Y. *et al.* Underlying burning resistant mechanisms for titanium alloy. *Materials & Design* **156**, 588-595 (2018).

24. *ASTM G124 Standard Test Method for Determining the Burning Behavior of Metallic Materials in Oxygen-Enriched Atmospheres, .* (ASTM, 2010).

25. Pilling, N. The oxidation of metals at high temperature. *J. Inst. Met.* **29**, 529-582 (1923).

26. Lee, J.-K. & Kim, S. K. Effect of CaO addition on the ignition resistance of Mg-Al alloys. *Materials transactions* **52**, 1483-1488 (2011).

27. Fassell Jr, W. M., Gulbransen, L. B., Lewis, J. R. & Hamilton, J. H. Ignition temperatures of magnesium and magnesium alloys. *JOM* **3**, 522-528 (1951).

28. Inoue, S., Yamasaki, M. & Kawamura, Y. Classification of high-temperature oxidation behavior of Mg-1 at% X binary alloys and application of proposed taxonomy to nonflammable multicomponent Mg alloys. *Corrosion Science* **174**, 108858 (2020).

29. Kim, Y. M., Yim, C. D., Kim, H. S. & You, B. S. Key factor influencing the ignition resistance of magnesium alloys at elevated temperatures. *Scripta Materialia* **65**, 958-961 (2011).

30. Lee, D. B. Effect of CaO and hot extrusion on the oxidation of AZ61 magnesium alloys. *Oxidation of Metals* **85**, 65-74 (2016).

31. Liu, M., Shih, D. S., Parish, C. & Atrens, A. The ignition temperature of Mg alloys WE43, AZ31 and AZ91.

Corrosion Science **54**, 139-142 (2012).
32. Kasprzak, W., Sokolowski, J., Sahoo, M. & Dobrzański, L. Thermal and structural characteristics of the AM50 magnesium alloy. *Journal of Achievements in Materials and Manufacturing Engineering* **28**, 131-138 (2008).
33. Nguyen, T. D. & Lee, D. B. Oxidation of AM60B Mg alloys containing dispersed SiC particles in air at temperatures between 400 and 550° C. *Oxidation of metals* **73**, 183-192 (2010).
34. Liu, C., Lu, S., Fu, Y. & Zhang, H. Flammability and the oxidation kinetics of the magnesium alloys AZ31, WE43, and ZE10. *Corrosion Science* **100**, 177-185 (2015).
35. Lee, D. B. High temperature oxidation of AZ31+0.3wt.%Ca and AZ31+0.3wt.%CaO magnesium alloys. *Corrosion Science* **70**, 243-251, doi:https://doi.org/10.1016/j.corsci.2013.01.036 (2013).
36. Cheng, S. Effect of Ca and Y additions on oxidation behavior of AZ91 alloy at elevated temperatures. *Transactions of Nonferrous Metals Society of China* **19**, 299-304 (2009).
37. Bobryshev, B. & Aleksandrova, Y. P. Ignition of magnesium and its alloys. *Metal Science and Heat Treatment* **30**, 219-222 (1988).
38. Wu, Y. *et al.* Ignition-proof properties of a high-strength Mg-Gd-Ag-Zr alloy. *Journal of Shanghai Jiaotong University (Science)* **17**, 643-647 (2012).
39. Zhou, N., Zhang, Z., Dong, J., Jin, L. & Ding, W. Selective oxidation behavior of an ignition-proof Mg-Y-Ca-Ce alloy. *Journal of Rare Earths* **31**, 1003-1008, doi:https://doi.org/10.1016/S1002-0721(13)60021-6 (2013).
40. Aydin, D., Bayindir, Z. & Pekguleryuz, M. The effect of strontium (Sr) on the ignition temperature of magnesium (Mg): a look at the pre-ignition stage of Mg–6 wt% Sr. *Journal of Materials Science* **48**, 8117-8132 (2013).
41. Tan, Q. *et al.* Generalisation of the oxide reinforcement model for the high oxidation resistance of some Mg alloys micro-alloyed with Be. *Corrosion Science* **147**, 357-371, doi:https://doi.org/10.1016/j.corsci.2018.12.001 (2019).
42. Fan, J. F. *et al.* Oxidation behavior of ignition-proof magnesium alloys with rare earth addition. *Journal of Alloys and Compounds* **509**, 2137-2142, doi:https://doi.org/10.1016/j.jallcom.2010.10.168 (2011).
43. Zhao, H., Zhang, Y. & Kang, Y. Effect of cerium on ignition point of AZ91D magnesium alloy. *Research & Development* (2008).
44. Lin, P. *et al.* Interactive effect of cerium and aluminum on the ignition point and the oxidation resistance of magnesium alloy. *Corrosion Science* **50**, 2669-2675 (2008).
45. Villegas-Armenta, L., Drew, R. & Pekguleryuz, M. The ignition behavior of Mg–Ca binary alloys: the role of heating rate. *Oxidation of Metals* **93**, 545-558 (2020).
46. Grosse, A. & Conway, J. Combustion of metals in oxygen. *Industrial & Engineering Chemistry* **50**, 663-672 (1958).
47. Wang, C. Microstructure and Combustion Characteristics of Aluminum-boron Alloy Powders. *Chinese Journal of Materials Science and Engineering* **39** (2021).
48. Gibbins, J., Stover, A., Krywopusk, N., Woll, K. & Weihs, T. Properties of reactive Al: Ni compacts fabricated by radial forging of elemental and alloy powders. *Combustion and Flame* **162**, 4408-4416 (2015).
49. Million, J. F. *et al.* Promoted Ignition-Combustion behavior of Cobalt and Nickel Alloys in Oxygen-Enriched Atmospheres. *J. ASTM Intl.* **6**, 10-20, doi:10.1520/JAI102230 (2009).
50. Hayun, S., Lilova, K., Salhov, S. & Navrotsky, A. Enthalpies of formation of high entropy and multicomponent alloys using oxide melt solution calorimetry. *Intermetallics* **125**, 106897, doi:https://doi.org/10.1016/j.intermet.2020.106897 (2020).

51. Liu, C., Lu, S., Cao, C. & Zhang, H. Experimental study on the effects of low air pressure on the magnesium alloy fires. *Joint Thermophysics and Heat Transfer Conference*, 3759 (2018).

52. Cheng, C. *et al.* Effect of Ca additions on ignition temperature and multi-stage oxidation behavior of AZ80. *Metals* **8**, 766 (2018).

53. Feng，Yunchao. *Investigation on the Ignition and Combustion of Aluminum/Aluminum-Magnesium Alloy Particle in Hot Gas* Master thesis, Graduate School of National University of Defense Technology (2019).

54. Sparks, K., Stoltzfus, J., Steinberg, T. & Lynn, D. Determination of burn criterion for promoted combustion testing. *Journal of the American Society for Testing and Materials (ASTM) International* **6**, 1-11 (2009).

55. Shao, L. *et al.* Combustion mechanism of alloying elements Cr in Ti-Cr-V alloys. *Materials* **12**, 3206 (2019).

56. Shao, L. *et al.* The effect of Cu content and Ti2Cu precipitation on the combustion behaviour and mechanism of Ti-xCu alloys. *Corrosion Science* **190**, 109641 (2021).

57. Yu, J. *et al.* Combustion behavior and mechanism of Cu46Zr46Al8 bulk metallic glass in oxygen-enriched environments. *Corrosion Science* **204**, 110415 (2022).

58. Ward, N. & Steinberg, T. The rate-limiting mechanism for the heterogeneous burning of cylindrical iron rods. *Journal of the American Society for Testing and Materials (ASTM) International* **6**, 1-13 (2009).

59. Yang, W. *et al.* Multiscale exploit the role of copper on the burn resistant behavior of Ti-Cu alloy. *Journal of Alloys and Compounds* **863**, 158639 (2021).

60. Zhang, W., Xu, P., Liang, D. & Liu, J. Thermal oxidation, ignition, and combustion characterization of AP-, LP-, and KN- coated multi-metal composite powders in Air/H2O environments. *Combustion and Flame* **271**, 113808, doi:https://doi.org/10.1016/j.combustflame.2024.113808 (2025).

61. Yang, Z.-j. *et al.* Combustion and energy release characteristics of Al/CuWO4 metal oxide-based thermite. *Ceramics International*, doi:https://doi.org/10.1016/j.ceramint.2025.06.054 (2025).

62. Wu, J. *et al.* Study on the influence of ignition voltage on the evaporation and combustion characteristics of metal nanofluid propellants. *Advances in Space Research* **77**, 2372-2388, doi:https://doi.org/10.1016/j.asr.2025.10.094 (2026).

63. Xu, P. *et al.* The role of bismuth trioxide in oxygen transport for enhancing combustion in a potential multi-metal aerial-aquatic fuel. *Combustion and Flame* **283**, 114583, doi:https://doi.org/10.1016/j.combustflame.2025.114583 (2026).

64. Wan, C. *et al.* A new ternary high-energy composite based on nano titanium powder with low sensitivity and stable combustion. *Combustion and Flame* **247**, 112480, doi:https://doi.org/10.1016/j.combustflame.2022.112480 (2023).

65. WebPlotDigitizer v. 5.2 (2024).

66. Wang, P., Ke, H. & Xue, Y. An integrated database of combustion properties of metallic materials. *Figshare*, doi:10.6084/m9.figshare.29966602 (2025).

67. Wang, P., Ke, H. & Xue, Y. CombustionData,GitHub repository, https://github.com/wpl2000/CombustionData (2026).

68. *NIST Chemistry WebBook https://webbook.nist.gov*.

69.Schneider, S.J., Compilation of the Melting Points Of the Metal Oxides, https://www.osti.gov/servlets/purl/4077673 (1963) .

70. Forsyth, E. T. *et al.* Development of Burn Curves to Assist With Metals Selection in Oxygen. *Flammability and*

Sensitivity of Materials in Oxygen-Enriched Atmospheres: 13th Volume **STP1561-EB**, doi:10.1520/stp20120018 (2012).

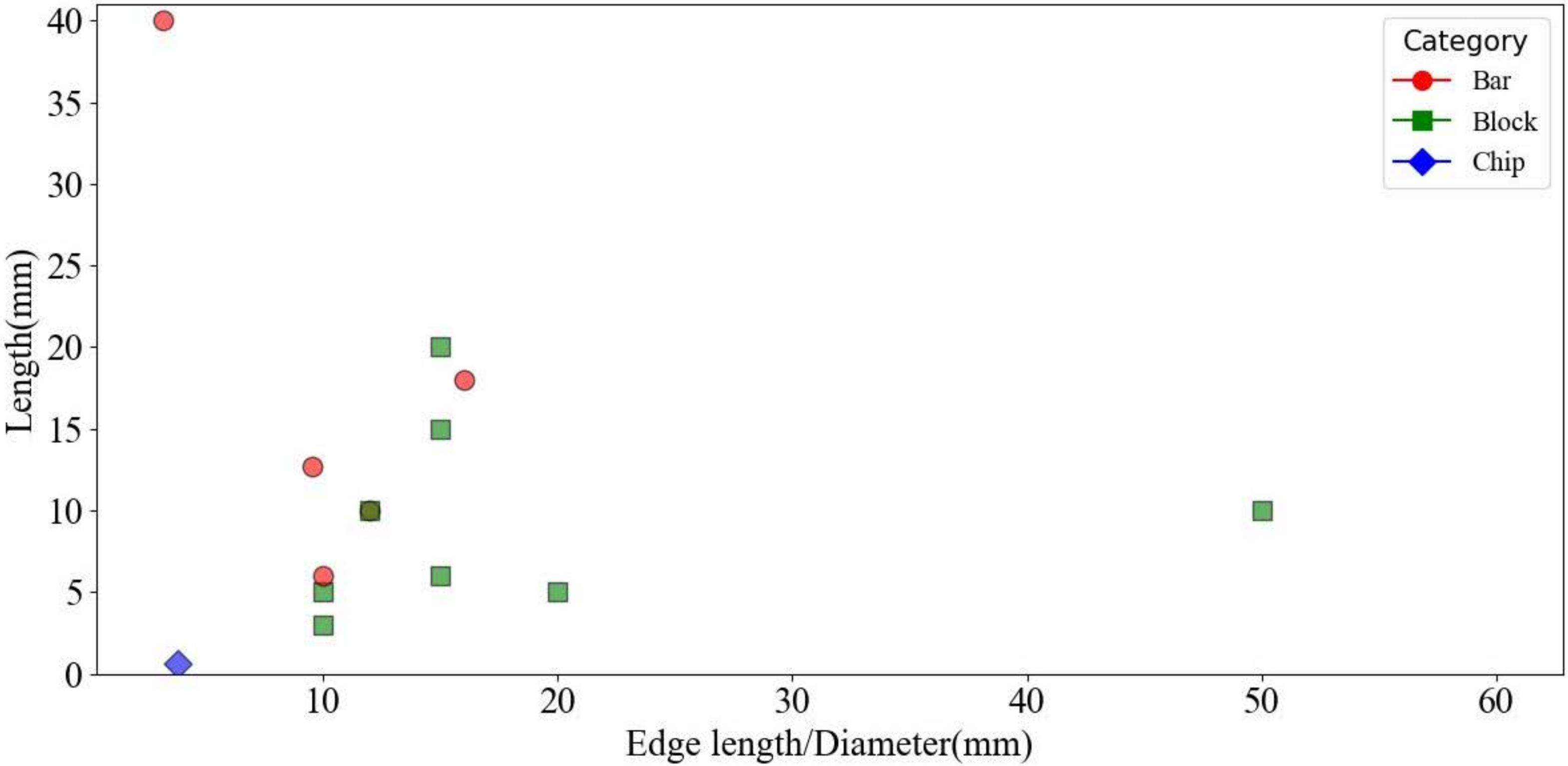

Category
Bar
Block
Chip
Length(mm)
Edge length/Diameter(mm)
0
5
10
15
20
25
30
35
40
10
20
30
40
50
60


Mg alloys
Ti alloys
Fe alloys
Al alloys
Pure metals
Ni alloys
Cu-Zr alloys
multi-conponent alloys
......
Combustion enthalpy
Ignition temperature
Ignition delay time
Combustion rate
Threshold pressure
Mg Cu Si Zr Al ...... ignition temperature(°C)
1 0 0 0 0 661.5969582
0.94 0 0 0 0.06 564.2585551
0.94 0 0 0 0 602.2813688
0.98 0 0 0 0 622.0532319
45 Papers
13 Material Classes
5 Combustion Metrics
725 Total Records

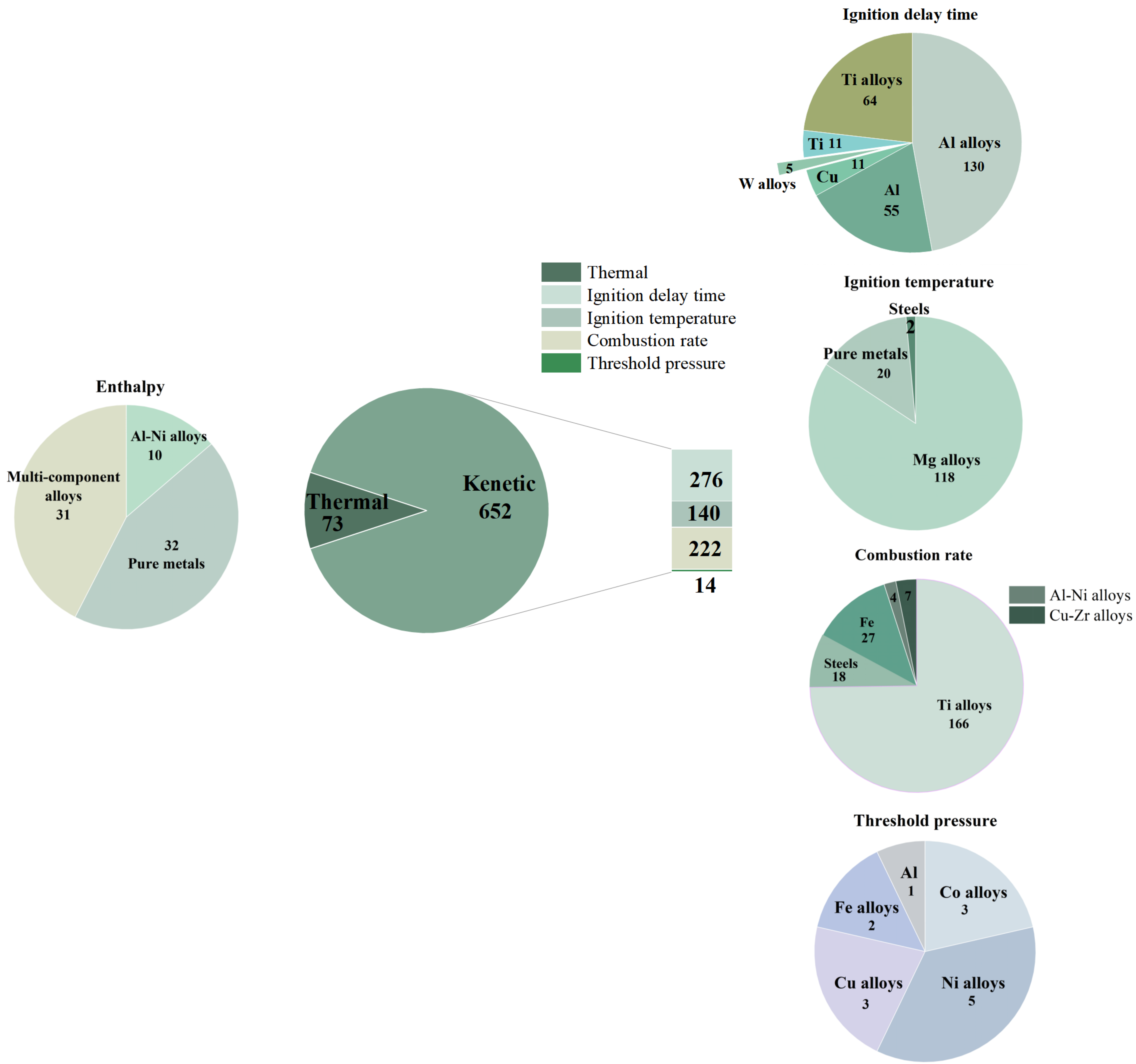
Ignition delay time
Ti alloys 64
Al alloys 130
Ti 11
5
W alloys
Cu
11
Al 55
Thermal
Ignition delay time
Ignition temperature
Combustion rate
Threshold pressure
Ignition temperature
Steels
2
Pure metals 20
Mg alloys 118
Enthalpy
Al-Ni alloys 10
Multi-component alloys 31
32 Pure metals
Thermal 73
Kenetic 652
276
140
222
14
Combustion rate
Al-Ni alloys
Cu-Zr alloys
Fe 27
4
7
Steels 18
Ti alloys 166
Threshold pressure
Al 1
Co alloys 3
Fe alloys 2
Cu alloys 3
Ni alloys 5

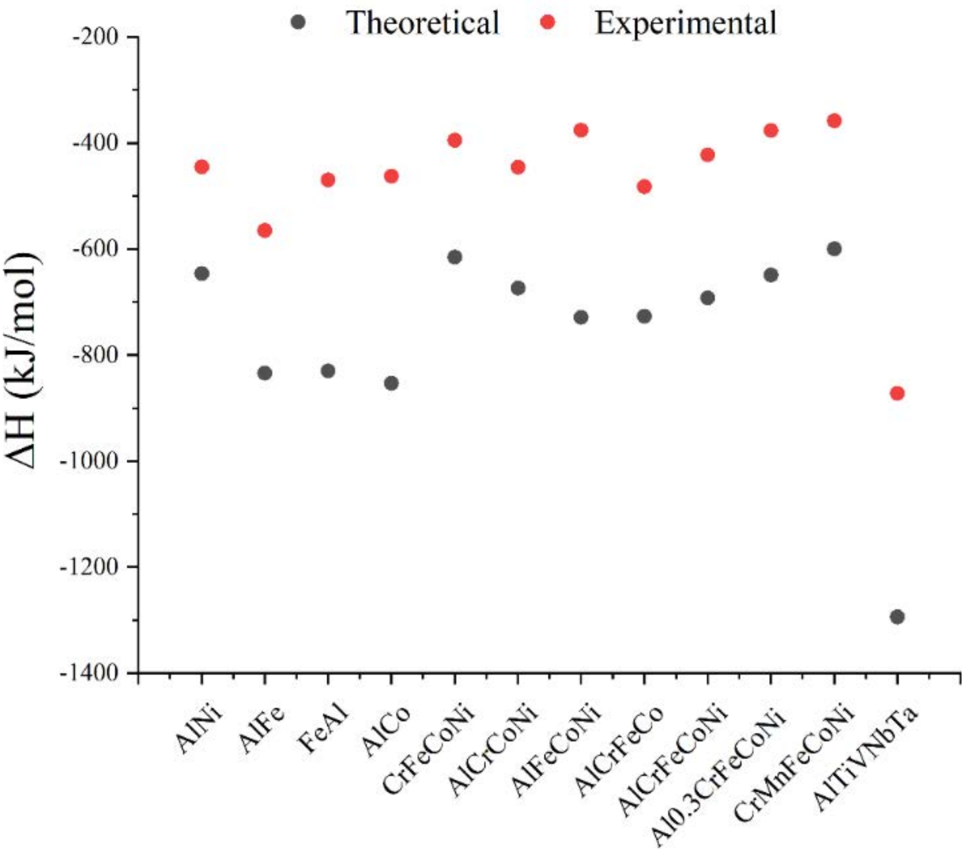
Theoretical
Experimental
ΔH (kJ/mol)
-200
-400
-600
-800
-1000
-1200
-1400
AlNi
AlFe
FeAl
AlCo
CrFeCoNi
AlCrCoNi
AlFeCoNi
AlCrFeCo
AlCrFeCoNi
Al0.3CrFeCoNi
CrMnFeCoNi
AlTiVNbTa

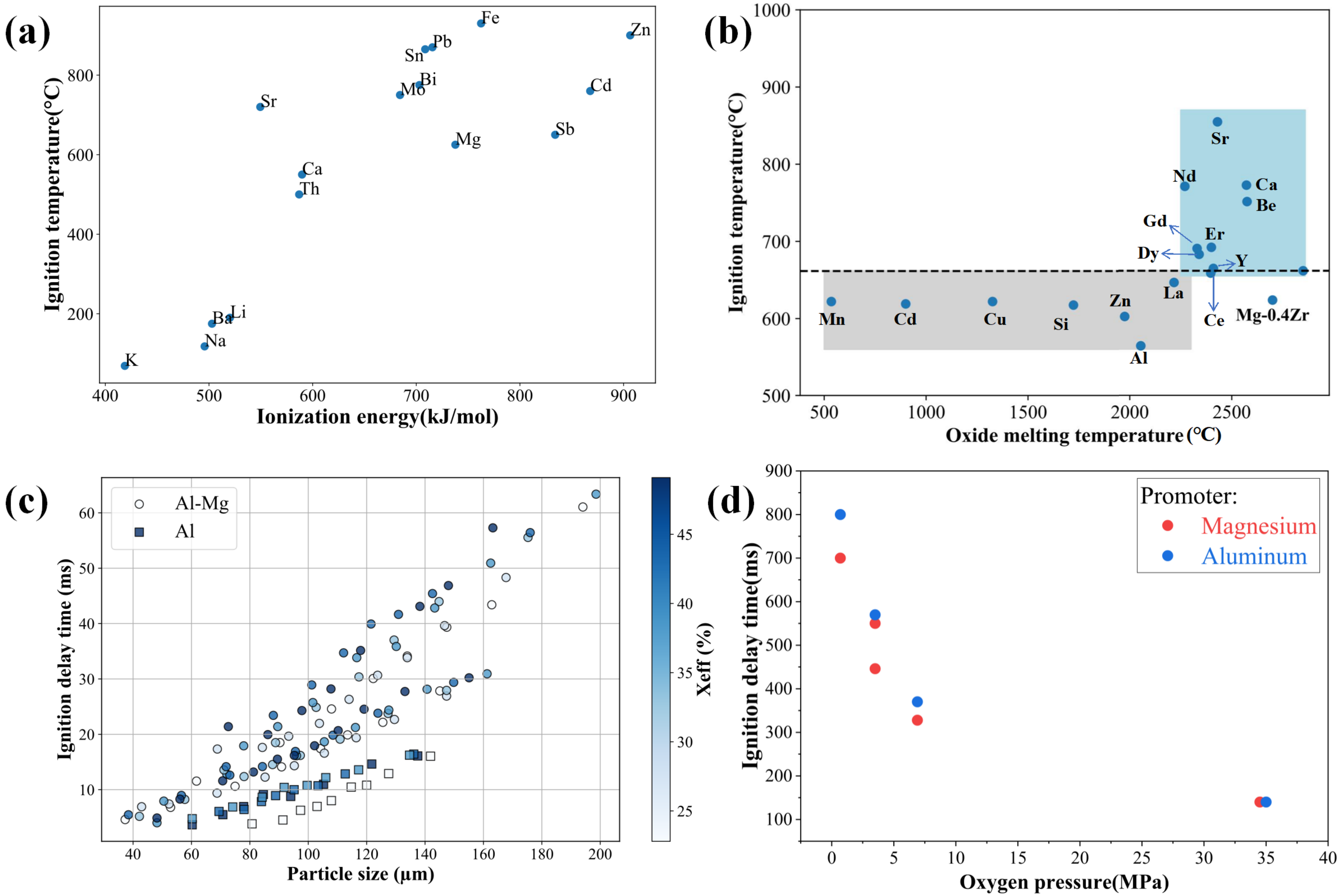
(a)
Ignition temperature(°C)
Ionization energy(kJ/mol)
K
Na
Ba
Li
Th
Ca
Sr
Mo
Bi
Sn
Pb
Fe
Mg
Sb
Cd
Zn
(b)
Ignition temperature(°C)
Oxide melting temperature (°C)
Mn
Cd
Cu
Si
Zn
Al
La
Ce
Mg-0.4Zr
Y
Dy
Gd
Er
Nd
Sr
Ca
Be
(c)
Al-Mg
Al
Ignition delay time (ms)
Particle size (μm)
Xeff (%)
(d)
Promoter:
Magnesium
Aluminum
Ignition delay time(ms)
Oxygen pressure(MPa)

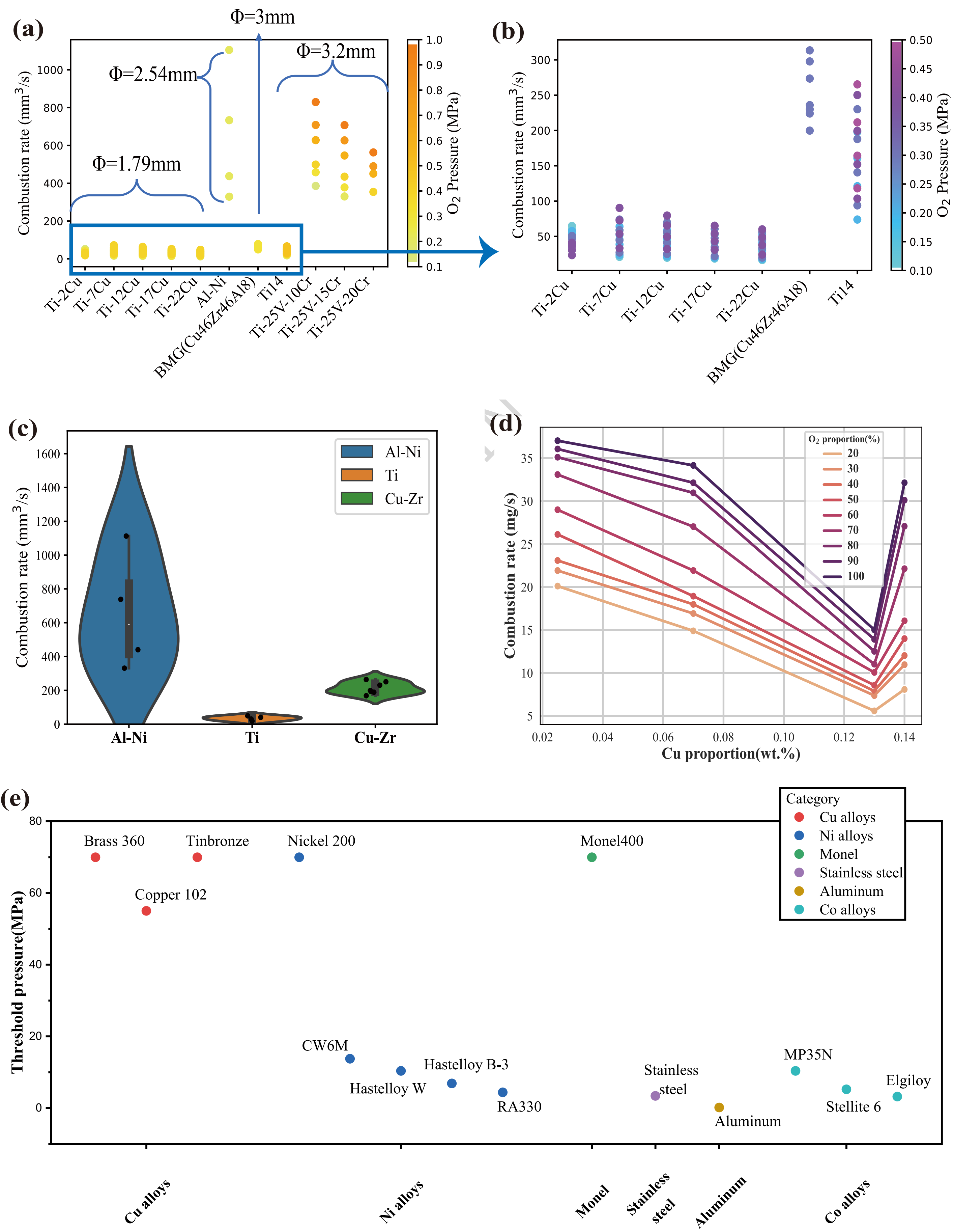

(a)
Φ=3mm
Φ=3.2mm
Φ=2.54mm
Φ=1.79mm
Combustion rate (mm³/s)
O₂ Pressure (MPa)
Ti-2Cu
Ti-7Cu
Ti-12Cu
Ti-17Cu
Ti-22Cu
Al-Ni
BMG(Cu46Zr46Al8)
Ti14
Ti-25V-10Cr
Ti-25V-15Cr
Ti-25V-20Cr
(b)
Combustion rate (mm³/s)
O₂ Pressure (MPa)
Ti-2Cu
Ti-7Cu
Ti-12Cu
Ti-17Cu
Ti-22Cu
BMG(Cu46Zr46Al8)
Ti14
(c)
Combustion rate (mm³/s)
Al-Ni
Ti
Cu-Zr
(d)
Combustion rate (mg/s)
Cu proportion(wt.%)
O₂ proportion(%)
20
30
40
50
60
70
80
90
100
(e)
Threshold pressure(MPa)
Category
Cu alloys
Ni alloys
Monel
Stainless steel
Aluminum
Co alloys
Brass 360
Tinbronze
Nickel 200
Monel400
Copper 102
CW6M
Hastelloy W
Hastelloy B-3
RA330
Stainless steel
Aluminum
MP35N
Stellite 6
Elgiloy
Cu alloys
Ni alloys
Monel
Stainless steel
Aluminum
Co alloys